BOREAL ENVIRONMENT RESEARCH 14: 45–55
ISSN 1239-6095 (print) ISSN 1797-2469 (online)

Helsinki 27 February 2009

Diurnal variability of precipitable water in the Baltic region, impact on transmittance of the direct solar radiation

Erko Jakobson[1)], Hanno Ohvril[1)] and Gunnar Elgered[2)]

[1)] *Institute of Environmental Physics, University of Tartu, Ülikooli 18, Tartu 50090, Estonia*
[2)] *Department of Radio and Space Science, Chalmers University of Technology, Onsala Space Observatory, SE-439 92 Onsala, Sweden*

Received 11 Oct. 2007, accepted 8 Feb. 2008 (Editor in charge of this article: Veli-Matti Kerminen)

Jakobson, E., Ohvril, H. & Elgered, G. 2009: Diurnal variability of precipitable water in the Baltic region, impact on transmittance of the direct solar radiation. *Boreal Env. Res.* 14: 45–55.

Diurnal variations in the Integrated Precipitable Water Vapour (IPWV) are studied from GPS observations acquired at 32 sites in the Baltic region during 1996–2005. The seasonal means for spring and summer show a diurnal sinusoidal pattern of the IPWV with the maximum value in the afternoon. The peak-to-peak (PtP) value of the average diurnal IPWV cycle was 0.5 mm in the spring and 0.6 mm in the summer. In the autumn and in the winter the diurnal variations in IPWV show no clear patterns and the average PtP values of the noise-like signal are only 0.2–0.3 mm. The diurnal IPWV cycle can only be estimated by averaging data from many years because the IPWV can show fast and large variations, reaching up to 5 mm/hour during several hours. These are explained exclusively by changes in the synoptic situation and substitution of airmasses above the location of observations; two case studies with analyses of the vertical humidity profiles are presented. The impact on the transmittance of the direct solar radiation is evaluated.

Introduction

The humidity content of the atmosphere, expressed as the integrated column of water vapour in the zenith direction, usually called integrated precipitable water vapour (IPWV), or just precipitable water (denoted W in equations and figures), is an important input to environmental models. The unit, mass per unit area, is in meteorological practice usually given as the thickness (height) of the layer of liquid water that would be formed if all the water vapour in the zenith direction were condensed at the surface of a unit area, hence 1-mm and 1-cm layers correspond to 1 kg m^{-2} and 1 g cm^{-2}, respectively (Reitan 1960, IPCC 2007).

Water vapour is the most important greenhouse gas, contributing to about 60% of the natural greenhouse effect; carbon dioxide accounts for just 26%, and ozone for 8% (Maurellis and Tennyson 2003). Water vapour also has a significant influence on accurate space geodesy applications (Beutler *et al*. 1988, Solheim *et al*. 1999), e.g. studies of crustal dynamics. In contrast to other greenhouse gases, water vapour has a much higher temporal and spatial variability which is not well observed, neither is it fully understood (Jacob 2001, Wagner *et al*. 2006).

The number of measurement techniques for observations of IPWV has increased considerably in 1990s and now includes ground-based and space-borne optical soundings and microwave

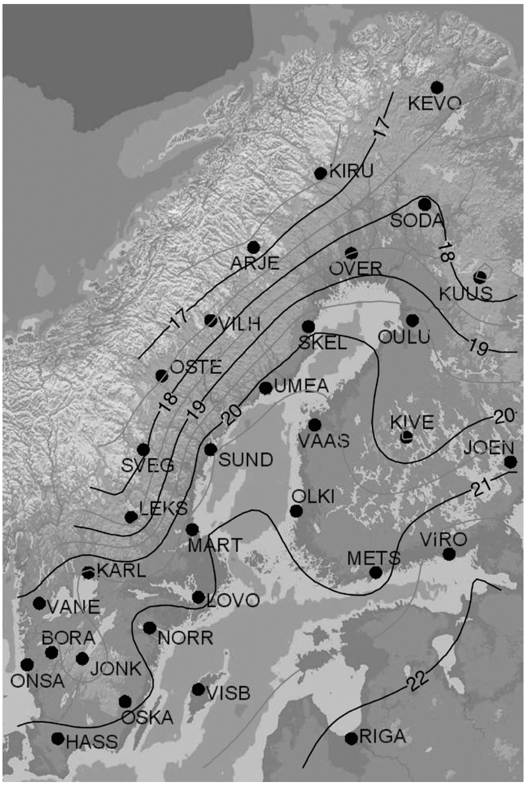

Fig. 1. GPS sites in the Baltic region from which data were acquired and analysed (21 Swedish stations (SWEPOS) in 1996–2005, 10 Finnish stations (FINNREF) in 1997–2005, 1 Latvian station (Riga) in 1998–2005). The summer (JJA) IPWV (mm) isolines are given.

radiometry, as well as propagation delay estimation using ground-based GPS data. The modern techniques enable a high temporal resolution (from seconds to minutes). It has been shown that GPS, radiosonde and microwave radiometer measurements of IPWV are in reasonable agreement with each other (Bouma and Stoew 2001, Güldner 2001, Dai *et al*. 2002).

In most countries, however, the classic balloon-borne radiosounding remains the main routine method for monitoring of IPWV. An advantage of this technique is of course that it provides profile information not only for water vapour but also for temperature and winds. This is the main method for long term studies of IPWV before 1990. Due to high costs, the network of radiosonde stations is sparse and sondes are launched usually only 1–2 times a day. The main launching time, 00:00 UTC, is for several stations the only one. Absence of reliable daytime IPWV observations seriously restricts interpretation of solar radiation and satellite observations (e.g. calculation of the water vapour attenuation of the direct solar radiation, transition from broadband to spectral optical parameters for atmospheric correction of satellite images, etc.) and raises a question about the diurnal pattern of IPWV. The support of interpretation of actinometric, AERONET (Aerosol Robotic Network, NASA) and satellite observations was the main motivation for this study (Kannel *et al*. 2007).

In this paper we introduce the GPS dataset and present the results estimated for the average diurnal variability of IPWV. We also analyse two extreme cases of abrupt IPWV variations, caused by the change of air masses above one of the locations of observations. Using the parametrization based on the SMARTS2 model (Gueymard 1995, 1998), we evaluate the impact of both average and extreme changes in IPWV on the transmittance of direct solar radiation

GPS data analysis

GPS data from 32 sites in the Baltic region were used (Fig. 1 and Table 1). The northernmost station is Kevo (69.76°N) and the southernmost is Hässleholm (56.09°N). From the longitudinal extent of stations, 18.2° (1 h 13 min) follows a ±37 min temporal variation of the local solar noon relative to the region's central meridian, 21°E, where the local noon is at 13:24 UTC.

The GPS data were analysed using two different strategies. The first one applied for the analysis of the diurnal variability is a so-called network solution using the GAMIT software developed at the Massachusetts Institute of Technology (King 2002). The processing used an elevation cut-off angle of 10° for the observations, the new mapping function (Niell 1996), and a temporal resolution of two hours for the estimated zenith total delay (ZTD). More details on this processing are given by Lidberg *et al*. (2007).

The other strategy is the Precise Point Positioning (PPP) technique (Zumberge *et al*. 1997), available within the GIPSY-OASIS software developed at the Jet Propulsion Laboratory (US) (Webb and Zumberge 1993), where each station

Table 1. The GPS sites used in the study. The IPWV yearly and seasonal averages (<*W*>) and PtP values of the diurnal signal.

No.	Code	Station	Lat. °N	Long. °E	<*W*> MAM	PtP MAM	<*W*> JJA	PtP JJA	<*W*> SON	PtP SON	<*W*> DJF	PtP DJF	<*W*> YEAR	PtP YEAR
1	HASS	Hässleholm	56.09	13.72	11.3	0.5	21.1	1.1	14.9	0.3	8.5	0.2	13.9	0.4
2	RIGA	Riga	56.95	24.06	10.9	1.0	22.2	1.1	14.1	0.5	7.7	0.4	13.7	0.5
3	OSKA	Oskarshamn	57.06	16.00	10.8	0.6	20.9	1.1	14.3	0.3	7.9	0.2	13.5	0.4
4	ONSA	Onsala	57.40	11.93	10.9	0.6	20.9	0.7	14.6	0.3	8.3	0.1	13.7	0.3
5	VISB	Visby	57.65	18.37	10.4	0.4	21.0	0.2	14.2	0.3	7.9	0.3	13.4	0.1
6	BORA	Borås	57.72	12.89	11.2	0.7	20.7	1.4	14.4	0.2	8.6	0.2	13.7	0.5
7	JONK	Jönköping	57.75	14.06	10.4	0.7	20.0	1.3	13.7	0.2	7.8	0.2	12.9	0.5
8	NORR	Norrköping	58.59	16.25	10.7	0.5	21.3	0.6	14.3	0.1	8.0	0.2	13.6	0.3
9	VANE	Vänersborg	58.69	12.07	10.5	0.6	20.1	1.2	14.0	0.2	8.1	0.1	13.2	0.4
10	LOVO	Lövö	59.34	17.83	10.3	0.6	20.9	0.4	14.0	0.2	7.9	0.2	13.3	0.2
11	KARL	Karlstad	59.44	13.51	10.5	0.8	20.6	0.7	14.1	0.2	8.0	0.2	13.3	0.3
12	METS	Metsähovi	60.22	24.40	9.5	0.6	20.7	0.7	12.7	0.4	7.1	0.4	12.5	0.3
13	VIRO	Virolahti	60.54	27.56	10.2	0.6	22.0	0.3	13.4	0.3	7.5	0.3	13.3	0.2
14	MART	Mårtsbo	60.60	17.26	10.0	0.5	20.9	0.7	13.5	0.1	7.5	0.2	13.0	0.3
15	LEKS	Leksand	60.72	14.88	8.8	0.7	18.1	0.8	11.9	0.2	6.7	0.3	11.4	0.3
16	OLKI	Olkilouto	61.24	21.47	9.9	0.5	20.9	0.9	13.5	0.2	7.4	0.2	12.9	0.3
17	SVEG	Sveg	62.02	14.70	8.5	0.4	17.8	1.0	11.5	0.4	6.5	0.2	11.1	0.3
18	SUND	Sundsvall	62.23	17.66	9.7	0.5	20.4	0.3	13.3	0.3	7.2	0.3	12.7	0.2
19	JOEN	Joensuu	62.39	30.10	9.1	0.7	20.9	0.7	12.2	0.7	6.5	0.3	12.2	0.3
20	KIVE	Kivetty	62.82	25.71	8.6	0.4	19.4	1.1	11.9	0.3	5.8	0.3	11.5	0.3
21	VAAS	Vaasa	62.96	21.77	9.5	0.6	20.8	1.0	13.3	0.5	7.3	0.3	12.7	0.3
22	OSTE	Östersund	63.44	14.86	8.3	0.4	17.4	0.9	11.2	0.4	6.5	0.2	10.9	0.3
23	UMEA	Umeå	63.58	19.51	9.2	0.7	20.2	0.6	12.8	0.3	7.0	0.2	12.3	0.3
24	VILH	Vilhelmina	64.70	16.56	8.0	0.4	17.4	0.6	11.1	0.4	6.3	0.2	10.7	0.2
25	SKEL	Skellefteå	64.88	21.05	8.8	0.7	19.9	0.7	12.4	0.4	6.6	0.2	11.9	0.3
26	OULU	Oulu	65.09	25.89	8.6	0.7	19.8	0.6	12.2	0.3	5.9	0.2	11.6	0.3
27	KUUS	Kuusamo	65.91	29.03	7.3	0.5	17.4	0.6	10.4	0.3	4.6	0.3	9.9	0.3
28	OVER	Överkalix	66.31	22.77	8.2	0.7	18.5	0.6	11.4	0.2	6.0	0.2	11.0	0.3
29	ARJE	Arjeplog	66.32	18.13	7.3	0.5	16.6	0.6	10.3	0.5	5.6	0.1	10.0	0.2
30	SODA	Sodankylä	67.42	26.39	7.8	0.6	18.1	0.6	11.0	0.5	5.3	0.3	10.6	0.2
31	KIRU	Kiruna	67.88	21.06	7.1	0.6	16.3	0.7	10.0	0.5	5.5	0.3	9.7	0.2
32	KEVO	Kevo	69.76	27.01	7.5	0.5	17.4	0.4	10.9	0.3	5.1	0.3	10.2	0.2
		Average	61.8	19.6	9.4	0.6	19.7	0.8	12.7	0.3	7.0	0.2	12.2	0.3
		SD			1.3	0.1	1.7	0.3	1.4	0.1	1.1	0.1	1.3	0.1

is processed individually. This requires accurate knowledge of the satellite orbits and clock errors, e.g. from a global network solution. This processing used the same mapping functions but an elevation cut-off angle of 15° and a temporal resolution of five minutes for the estimated ZTD. We used this dataset, produced by Johansson *et al*. (2002), for the case studies of fast IPWV variations at Onsala.

The part of the ZTD caused by water vapour, the zenith wet delay (ZWD), was derived by subtracting the so-called zenith hydrostatic delay (ZHD) using values of the ground pressure interpolated from a numerical weather analysis as described by Gradinarsky *et al*. (2002). The conversion from ZWD to the IPWV used the model presented by Emardson and Derks (2000) which is based on the season (day of year) and the latitude of the site.

The uncertainties in the IPWV values have many origins and span from white noise in fundamental carrier-phase observations to long term bias effects due to uncertainties in physical constants used in the conversions described above. A total root-sum-square error of GPS measured IPWV has been shown to be slightly above the 1-mm level when using data from the Swedish and Finnish networks (Emardson *et al*. 1998) and from Tasmania, Australia (Tregoning *et al*. 1998).

Here we focuse on the diurnal variability, meaning that long-term systematic effects with time scales much longer than a day can be ignored. The influence of white-noise errors were effectively averaged out. More difficult systematic errors with time scales of around a day, such as tidal effects, effect of ocean loading and orbit errors of GPS satellites, are reduced when averages are formed using several years of data. In fact, since the PtP of the IPWV in the studied area was typically well below the 1-mm level, the detection of the diurnal cycles required that averages over several years were formed.

The average diurnal variability of IPWV

Factors influencing the diurnal changes of IPWV can be divided into two groups. The fast and extensive but irregular IPWV variations are due to changes in synoptic situation and the substitution of air masses above the GPS site leading to rapid and large (more than 10 mm) variations in the vertical profiles of water vapour. The very rapid changes are, however, not so frequent. For example, during only about 1% of the days at Onsala, there was a change in IPWV that was larger than 10 mm during six hours. Small, regular diurnal variations of IPWV are driven by the diurnal cycle of solar radiation linked with the evapotranspiration processes in the atmosphere and on the underlying surface, and by local air circulation. In this section we present the averaged diurnal patterns representing regular diurnal variations of IPWV.

In order to study the seasonal dependence of the regular diurnal variations in IPWV, we divided the dataset into the four seasons: spring (MAM), summer (JJA), autumn (SON) and winter (DJF). For each of $N = 32$ stations we calculated its average diurnal evolution of IPWV, $W_{\mathrm{St,UTC}}$, where the index St marks a station and the index UTC time with a step of two hours: UTC = 00:00, 02:00, ..., 22:00. Next we found station diurnal anomaly, $\Delta W_{\mathrm{St,UTC}}$, for each of $M = 12$ hours, as the difference from the station daily mean, W_{St}:

$$\Delta W_{\mathrm{St,UTC}} = W_{\mathrm{St,UTC}} - W_{\mathrm{St}}. \qquad (1)$$

In the spring and in the summer the average diurnal anomaly ΔW_{UTC} had a regular, almost sinusoidal pattern (black lines in Fig. 2). In the spring and in the summer the average daily cycle peaked at 14:00 UTC (about 15:20 Local Solar Time at the region's central meridian, 21°E) and exceeded the daily mean by only 0.25 mm in the spring and by 0.33 mm in the summer (Table 2). The lowest IPWV values occurred typically between 00:00 and 04:00 UTC. They were 0.26 and 0.31 mm below the daily-mean values in the spring and summer, respectively.

In order to study the IPWV scatter about its average diurnal cycle, we calculated the seasonal standard deviation (SD) as follows:

$$\mathrm{SD}(\Delta W) = \sqrt{\frac{1}{N \times M - M} \sum_{\mathrm{St}=1}^{N} \sum_{\mathrm{UTC}=1}^{M} \left(\Delta W_{\mathrm{St,UTC}} - \Delta W_{\mathrm{UTC}}\right)^2}, \qquad (2)$$

where the sums were taken over all stations ($N =$

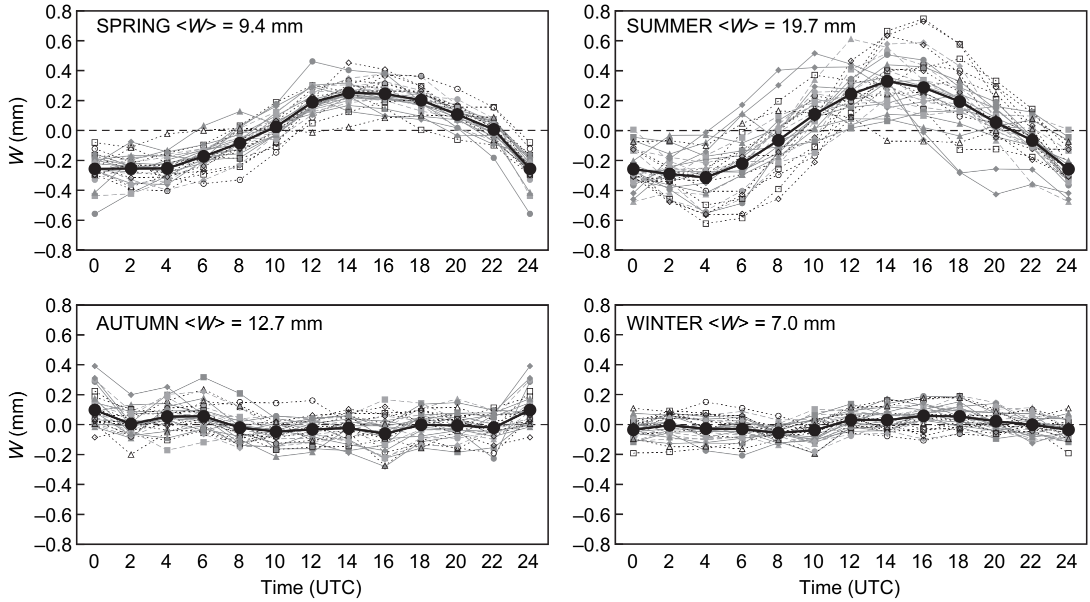

Fig. 2. Grey lines: the IPWV seasonal mean diurnal anomalies for the 32 GPS stations. Black lines: averages over all the 32 stations; <*W*> is the seasonal average of IPWV for the region (over all stations and hours).

32) and hours ($M = 12$). The denominator, $N \times M - M$, expresses the number of degrees of freedom in the process of averaging.

SD(ΔW) was only 0.08 mm in the spring and 0.16 mm in the summer. These values are small as compared with the average values of PtP (0.51 mm for the spring and 0.64 mm for the summer). Thus in the spring and summer, the average diurnal cycle of IPWV could be used instead of a station's individual one.

The average diurnal PtP value of IPWV was 0.16 mm in the autumn and 0.11 mm in the winter. Apparently, smaller amplitude in the diurnal variation of incoming radiation and larger values of cloudiness in the autumn and winter as compared with those in the other seasons smoothed both the temperature and humidity differences between day and night, and therefore also the diurnal humidity cycles. The value of STDEV(ΔW) was 0.09 mm in the autumn and 0.07 mm in the winter. We conclude that it seems reasonable to neglect the diurnal cycles in the IPWV during the autumn and winter seasons.

Bouma and Stoew (2001) found that the average PtP values of IPWV using GPS observations from almost the same area were larger: 1.1 mm in the summer and 0.8 mm in the winter. One explanation for these differences can be the shorter time span of the database used by Bouma and Stoew (2001) — from January 1997 until August 1999. This period was apparently too short to smooth out individual fast changes in IPWV during front passages and corresponding substitution of air masses. For example, we calculated the PtP values of IPWV for a particular station, Jönköping, with reduced temporal extension of observations, from January 1997 to August 1999, like in Bouma and Stoew (2001).

Table 2. Seasonal average diurnal evolutions of the IPWV anomalies (mm).

	00	02	04	06	08	10	12	14	16	18	20	22	PtP
MAM	–0.26	–0.26	–0.25	–0.17	–0.08	0.02	0.19	0.25	0.25	0.20	0.11	0.01	0.51
JJA	–0.26	–0.29	–0.31	–0.22	–0.07	0.11	0.24	0.33	0.29	0.19	0.05	–0.07	0.64
SON	0.10	0.00	0.05	0.06	–0.02	–0.05	–0.03	–0.02	–0.06	0.00	–0.01	–0.02	0.16
DJF	–0.03	–0.01	–0.03	–0.03	–0.06	–0.04	0.03	0.03	0.06	0.05	0.02	0.00	0.11

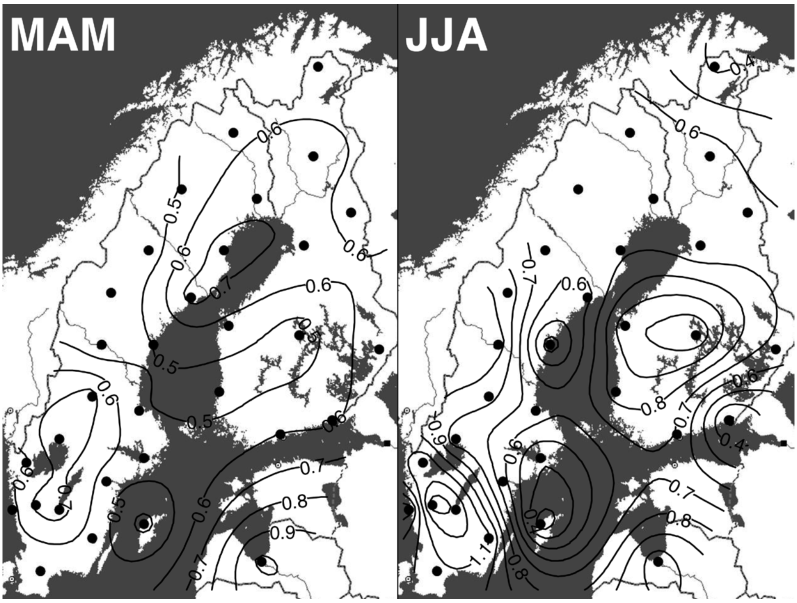

Fig. 3. The IPWV (mm) diurnal average PtP values for the spring (MAM) and for the summer (JJA).

As compared with those for the period 1996–2005, the PtP values increased in the summer from 1.3 to 1.6 mm and in the winter from 0.2 to 0.4 mm (Table 1). The PtP values for Jönköping given by Bouma and Stoew (2001) were 1.5 mm in the summer and 0.8 mm in the winter. The residual discrepancy between the results by Bouma and Stoew (2001) and those by our 2.5-year data set can be explained with different methods for the calculation of the initial IPWV database (cut-off angle, algorithms) and with different temporal averaging intervals. Bouma and Stoew (2001) used 1-hour intervals, from which (due to a higher temporal resolution) slightly higher PtP values followed as compared with our 2-hour interval.

Maps with IPWV PtP isolines for the spring and summer are shown in Fig. 3. We do not show similar maps for the autumn and winter because the PtP values were too small and noise-like.

The largest PtP variations of IPWV were observed for the inland stations in southwestern Sweden, supposedly because of the lower latitude and sufficient distance from the sea that enables larger diurnal variability in the temperature. In Riga, there were also large variations in PtP, explained apparently also with its lower latitude. Minimal PtP variations, explained by the mitigation by sea, were observed for the only island station Visby. Due to the overall small summer IPWV values in the northernmost station Kevo, the diurnal amplitude there was also small. It is interesting to note that compared with the western coast, the summer PtP variations were slightly larger at the more continental eastern coast of the Gulf of Bothnia.

Extreme cases of fast IPWV variations at Onsala

9 September 1999

During 5 hours and 25 minutes (16:57–22:22 UTC), the IPWV decreased from 35 to 10 mm, i.e. by 25 mm, with an average trend of about 5 mm hour^{-1} (Fig. 4a). This drop can be explained by the substitution of air masses over Onsala. Vertical profiles of the specific humidity, q (g kg^{-1}), for 18:00 and 00:00 UTC obtained at the vicinity of the Landvetter airport (distance 37 km) showed that during these six hours, the humidity content decreased in the entire profile, especially between 1 and 4 km (Fig. 5a).

The NOAA HYSPLIT model (http://www.arl.noaa.gov/ready/hysplit4.html) backward trajectories demonstrated the different origin of air masses over Onsala. At 18:00 UTC before the

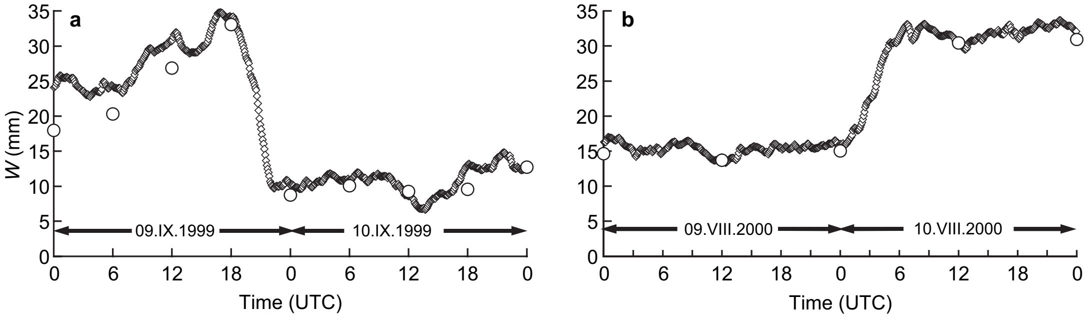

Fig. 4. (**a**) Rapid decrease in the IPWV on 9 September 1999 and (**b**) increase on 10 August 2000. Diamonds (seen as almost continuous lines) represent GPS measured IPWV at the Onsala site with a temporal resolution of 5 min; circles denote IPWV measured by radiosondes at the Landvetter airport.

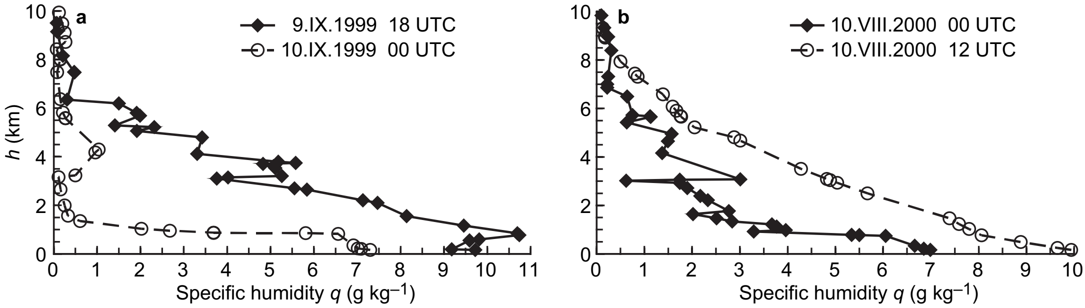

Fig. 5. Vertical profiles of the specific humidity q (g kg^{-1}) at the Landvetter airport. Diamonds (connected with solid lines) show the earlier profiles before the substitution of air masses, circles (dashed lines) show the profiles for the new air masses.

fast change, hot air with a high humidity content originated from western Europe. Afterwards at 24:00 UTC, cold air with a low humidity content originated from Greenland, Iceland and the North Atlantic region.

10 August 2000

During 6 hours and 20 minutes (00:27–06:47 UTC), the IPWV increased from 16 to 33 mm, i.e. by 17 mm, with an average trend of about 3 mm hour^{-1} (Fig. 4b). Vertical profiles of the specific humidity, q, for 00:00 and 12:00 UTC obtained at the Landvetter airport showed that during these 12 hours, the humidity content increased along the entire profile (Fig. 5b). This increase can also be explained by a long-range transport of air masses: warmer and humid air from western Europe pushed out previous colder and drier air from Greenland, Iceland and the North Atlantic region.

Impact of changes in the IPWV on absorption of solar radiation

Here we address the following question: how the observed changes in the IPWV affect the transmittance of the broadband direct solar radiation? In order to answer this question, we have to use some kind of a model for determination of absorption of solar radiation during its passage through a hypothetical atmosphere consisting of water vapour only. There are two difficulties involved in this kind of modelling. The first is complexity of the extraterrestrial solar spectrum. The second is peculiarity of the water vapour molecule, leading to a complicated vibration-rotation absorption spectrum. Although high-resolution molecular spectroscopy can measure the wavelengths of absorption lines, the problem is in the intensity of these lines. Water molecules form droplets and stick to the walls of tubes, so they do not mix properly with other gases. Therefore, the concentration of water vapour is diffi-

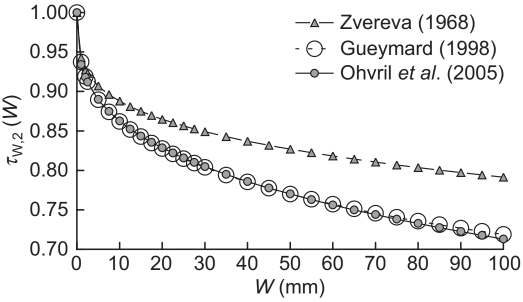

Fig. 6. Transmittances of water vapour for broadband direct solar radiation at atmospheric optical mass m = 2 (corresponds to solar elevation ≈ 30°) as functions of the IPWV in the zenith direction, W (mm).

cult to be controlled in an experiment, making it troublesome to perform validation measurements (Maurellis and Tennyson 2003). During the last decades, however, progress has been made in models calculating the water vapour attenuation of the solar radiation, leading to larger values of absorption. The last statement follows, for example, from comparing parametrizations proposed by Zvereva (1968) and Gueymard (1998).

For the calculation of extinction of solar radiation, we used the parametrization proposed by Gueymard (1995, 1998) which is based on his model SMARTS2 for atmospheric radiative transfer of sunshine. He used a solar spectrum of 1881 wavelengths, at 1-nm intervals within the most important part of the spectrum (280–1700 nm). Although the parametrization consists of 20 formulas, it was demonstrated by Ohvril *et al*. (2005) that in a particular case, for atmospheric optical mass m = 2 (corresponding to a solar elevation angle of about 30°), the transmittance of water vapour $\tau_{W,2}$ can be expressed with a single formula:

$$\tau_{W,2}(W) = 1 - 0.0657W^{0.32}, \quad (3)$$

where W is the IPWV in the zenith direction expressed in mm and the index "2" indicates the number of atmospheric optical masses, m = 2, in the sun's direction.

Plots of transmittances $\tau_{W,2}$ — calculated according to Zvereva (1968), Gueymard (1998) and Ohvril *et al*. (2005) — are given in Fig. 6 as functions of IPWV in the zenith direction. Two results are evident: (1) the approximation (Eq. 3) provides an excellent agreement with the parametrization by Gueymard (1998), and (2) the method by Gueymard (1998) gives considerably stronger attenuation of direct radiation than that by Zvereva (1968).

By inserting the seasonal average IPWV values for spring and summer (9.4 mm and 19.7 mm respectively) into Eq. 3 we obtain transmittances for solar radiation: 0.86 for the spring and 0.83 for the summer. Interpreting now diurnal average PtP values — 0.51 mm for the spring and 0.64 mm for the summer — as anomalies from seasonal averages, from Eq. 3 we see that transmittances change only by 0.27% in the spring and 0.20% in the summer. The largest average diurnal change in the summer occurred in Borås (Table 1): PtP = 1.4 mm and W = 20.7 mm, which gives a change of 0.47% in transmittance. These changes are of the same order of magnitude as the errors in high quality observations of the direct solar radiation — the uncertainty of a well-calibrated pyrheliometer is at the 95% confidence level about 0.5% (Thacher 2000). However, according to practice of Estonian Meteorological and Hydrological Institute, error of actinometers (operational instruments for continuous everyday measurements of direct solar beam) is larger, reaching 4%. Consequently, the average summer diurnal change in transmittance, caused by changes in IPWV, is smaller as compared with errors in observation of the direct radiation.

The situation is different when analysing extreme changes in the IPWV. For example, the detected abrupt drop by 25 mm in the IPWV on 9 September 1999 at Onsala produced an increase in the transmittance of the direct solar radiation of 9%. The sudden increase by 17 mm in the IPWV on 10 August 2000 produced a decrease in the transmittance of 5%. Therefore, short-term changes in the IPWV, caused by substitution of air masses above the location of observation, affect the transmittance to a greater extent than do the observational errors of the direct solar radiation.

Conclusions

The necessity for better geographical and temporal presentation of IPWV in atmospheric studies is highlighted by the disturbing fact that atmospheric models underestimate absorption of sunlight (Maurellis and Tennyson 2003). A probable explanation for "the surplus radiation" in the global energy budget, besides underestimation of absorption by water vapour in the optical and UV region, may be hidden by an insufficient representation of the planetary distribution of the IPWV considering also its temporal variability (Jakobson *et al*. 2005).

We studied diurnal variations in the IPWV by analysing 2-hour averaged data for a period 1996–2005 derived from GPS observations at 32 sites in the Baltic region. The average seasonal values over all stations were 9.4 mm for the spring, 19.7 mm for the summer, 12.7 mm for the autumn and 7.0 mm for the winter. Atmospheric optical models often use fixed values of IPWV for certain climatic conditions. For example, the MODTRAN models (Qiu 2001) use six values of the IPWV: 41.2 mm (tropical), 29.3 mm (midlatitude summer), 20.8 mm (subarctic summer), 14.2 mm (the 1976 U.S. Standard Atmosphere), 8.5 mm (midlatitude winter) and 4.1 mm (subarctic winter). The summer average value (19.7 mm) obtained from our database is close to the MODTRAN subarctic summer value but lower than the most recent estimate of the planetary mean IPWV of 24.9 mm (Trenberth and Smith 2005). Our spring IPWV (9.4 mm) corresponds to midlatitude winter (8.5 mm). However, our winter IPWV of 7.0 mm is considerably higher than its MODTRAN subarctic counterpart of 4.1 mm.

It should be noted that the used set of GPS stations do not cover the southern part of the Baltic drainage area, in which the atmospheric humidity content is generally higher: as shown in a study of radiosonde observations (launched only 1–2 times daily), seasonal averages for the stations Greifswald, Legionowo, Lindenberg and Wroclav, having latitudes 52–54°N, are in a range IPWV = 22–24 mm in the summer, 16–17 mm in the autumn, 13–14 mm in the spring and 9–10 mm in the winter (Jakobson *et al*. 2005).

Diurnal variations of IPWV can be divided into two groups: the large irregular and small regular ones. The large variations in IPWV are related to changes in the synoptic situation and the substitution of air masses above the location of observations. As shown by the analysis of two extreme examples of abrupt changes in atmospheric humidity at the Onsala site, the IPWV total increase/decrease can reach even 25 mm during six hours. Concerning the Onsala site, during only about 1% of days there was a change in the IPWV that was larger than 10 mm during six hours.

The average diurnal variability of the IPWV in the Baltic region between 56°N and 70°N is low, the maximal average station PtP value in the summer being 1.4 mm at Borås. The seasonal mean diurnal variation of IPWV has a sinusoidal pattern in the spring and in the summer with the maximum at afternoon and the minimum after midnight. The PtP value, for the region average IPWV cycle, is 0.5 mm in the spring and 0.6 mm in the summer. Regular diurnal variations of IPWV are without a definite pattern in the autumn and in the winter, PtP values of the average IPWV cycle are only 0.1–0.2 mm.

Concerning interpretation of solar radiation observations in the region, the average diurnal variations in the IPWV, extending 1.4 mm in the summer, produces changes in the transmittance of the broadband direct solar radiation of less than 0.5%. The changes in the synoptic situation expressed by substitution of air masses above the location of solar radiation measurements can produce changes in transmittance extending up to 9%.

Summarising, as a result of the analysis, we have a quantitative picture on the diurnal behaviour of the IPWV in the Baltic area. Concerning atmospheric radiation studies, we have now information on admissibility and dangers in the usage of nighttime IPWV values instead of the daytime ones. As usual, new problems have been identified: (1) why do the minimal IPWV values occur between 00:00 and 04:00 UTC and not exactly before sunrise in the spring and in the summer, and (2) why the IPWV, for particular locations (Metsähovi, Vaasa) peaks already at 10:00 UTC? In order to answer these questions, detailed information on diurnal changes in the water vapour density is needed in the entire vertical profile. It means that radiosounding campaigns with a launching interval about 2–3 hours are needed.

Acknowledgements: We thank Lars Mueller at the Swedish Meteorological and Hydrological Institute (SMHI) for providing the ground meteorological data. We are also grateful to Martin Lidberg and Jan Johansson at Chalmers for making their ZTD time series from the GAMIT and GIPSY GPS solutions available. The NOAA HYSPLIT team is highly appreciated for making the unique trajectory calculations available. The Estonian Science Foundation has supported the investigation by the national grant No. 5857 and 7347. The Swedish National Space Board has supported the research on GPS meteorology at Chalmers.

References

Beutler G., Bauersima I., Gurtner W., Rothacher M., Schildknecht T. & Geiger A. 1988. Atmospheric refraction and other important biases in GPS carrier phase observations. In: Brunner F.K. (ed.), *Atmospheric effects on geodetic space measurements*, Monograph 12, School of Surveying, University of N.S.W., Sydney, pp. 15–43.

Bouma H.R. & Stoew B. 2001. GPS observations of daily variations in the atmospheric water vapor content. *Phys. Chem. Earth A* 26: 389–392.

Dai A., Wang J., Ware R.H. & Hove T. 2002. Diurnal variation in water over North America and its implications for sampling errors in radiosonde humidity. *J. Geophys. Res.* 107, doi:10.1029/2001JD000642.

Emardson T.R., Elgered G. & Johansson J. 1998. Three months of continuous monitoring of atmospheric water vapor with a network of Global Positioning System receivers. *J. Geophys. Res.* 103: 1807–1820.

Emardson T.R. & Derks H.J.P. 2000. On the relation between wet delay and the integrated precipitable water vapour in the European atmosphere. *Meteorol. Appl.* 7: 61–68, doi:10.1017/S1350482700001377.

Gradinarsky L.P., Johansson J.M., Bouma H.R., Scherneck H.-G. & Elgered G. 2002. Climate monitoring using GPS. *Phys. Chem. Earth* 27: 335–340.

Gueymard C. 1995. *SMARTS2, a simple model of the atmospheric radiative transfer of sunshine: algorithms and performance assessment*, Tech. Rep. FSEC-PF-270-95. [Available from Florida Sol. Energy Center, 1679 Clearlake Rd., Cocoa, FL 32922-5703, USA].

Gueymard C. 1998. Turbidity determination from broadband irradiance measurements: a detailed multicoefficient approach. *J. Appl. Meteor.* 37: 414–435.

Güldner J. 2001. Validation of integrated water vapor using independent measurement techniques. *Phys. Chem. Earth A* 26: 427–431.

IPCC 2007. *Climate change 2007: the physical science basis. Contribution of working group I to the fourth assessment report of the intergovernmental panel on climate change*. Cambridge University Press, Cambridge, United Kingdom and New York, NY, USA.

Jacob D. 2001. The role of water vapour in the atmosphere. A short overview from a climate modeller's view. *Phys. Chem. Earth A* 26: 523–527.

Jakobson E., Ohvril H., Okulov O. & Laulainen N. 2005. Variability of radiosonde-observed precipitable water in the Baltic region. *Nordic Hydrology* 36: 423–433.

Johansson J.M., Davis J.L., Scherneck H.-G., Milne G.A., Vermeer M., Mitrovica J.X., Bennett R.A., Jonsson B., Elgered G., Elosegui P., Koivula H., Poutanen M., Rönnäng B.O. & Shapiro I.I. 2002. Continuous GPS measurements of postglacial adjustment in Fennoscandia 1. Geodetic results. *J. Geophys. Res.* 107, doi:10.1029/2001JB000400.

Kannel M., Ohvril H., Teral H., Russak V. & Kallis A. 2007. A simple parameterization of columnar aerosol optical thickness. *Proc. Estonian Acad. Sci. Biol. Ecol.* 56: 57–68.

Lidberg M., Johansson J.M., Scherneck H.-G. & Davis J.L. 2007. An improved and extended GPS-derived 3D velocity field of the glacial isostatic adjustment (GIA) in Fennoscandia. *J. Geodesy* 81: 213–230, doi: 10.1007/s00190-006-0102-4.

Maurellis A. & Tennyson J. 2003. *The climatic effects of water vapor*. Available at http://physicsworld.com/cws/article/print/17402.

Niell, A.E. 1996. Global mapping functions for the atmosphere delay at radio wavelengths. *J. Geophys. Res.* 101: 3227–3246.

Ohvril H., Teral H., Tee M., Russak V., Okulov O., Jõeveer A., Kallis A., Abakumova G., Terez E., Guschchin G., Terez G., Olmo F.J., Alados-Arboledas L. & Laulainen N. 2005. Multi-annual variability of atmospheric transparency in Estonia. In: *SOLARIS 2005 — 2nd Joint Conference. International Forum of Experts in Solar Radiation*, Hellenic Illumination Committee, Athens, pp. 42–46.

Qiu J. 2001. Broadband extinction method to determine atmospheric optical properties. *Tellus* 53B: 72–82.

Reitan C.H. 1960. Mean monthly values of precipitable water over the United States, 1946–56. *Mon. Weath. Rev.* 88: 25–35.

Solheim F.S., Vivekanandan J., Ware R.H. & Rocken C. 1999. Propagation delays induced in GPS signals by dry air water vapor, hydrometeors, and other particulates. *J. Geophys. Res.* 104: 9663–9670.

Thacher P.D., Boyson W.E. & King D.L. 2000. Investigation of factors influencing the accuracy of pyrheliometer calibrations. *Photovoltaic Specialists Conference/IEEE Electron Devices Society*: 1395–1398, doi:10.1109/PVSC.2000.916153.

Tregoning P., Boers R., O'Brien D. & Hendy M. 1998. Accuracy of absolute precipitable water vapor estimates from GPS observations. *J. Geophys. Res.* 103: 701–710.

Trenberth K.E. & Smith L. 2005. The mass of the atmosphere: a constraint on global analyses. *J. Climate* 18: 864–875.

Wagner T., Beirle S., Grzegorski M. & Platt U. 2006. Global trends (1996–2003) of total column precipitable water observed by Global Ozone Monitoring Experiment (GOME) on ERS-2 and their relation to near-surface temperature. *J. Geophys. Res.* 111, D12102, doi:10.1029/2005JD006523.

Webb F.H. & Zumberge J.F. 1993. *An introduction to the GIPSY/OASIS-II*. Jet Propulsion Lab, JPL Publ. D-11088.

Zumberge J.F., Heflin M.B., Jefferson D.C., Watkins M.M., & Webb F.H. 1997. Precise point positioning for the efficient and robust analysis of GPS data from large networks. *J. Geophys. Res.* 102: 5005–5017.

Zvereva S.V. [Зверева С.В.] 1968. [On the absorption of solar radiation by atmospheric water vapor]. In: [*Actinometry and atmospheric optics. Reports of the sixth interdepartmental symposium on actinometry and atmospheric optics, June 1966, Tartu*], Valgus, pp. 117–121. [In Russian].